Materials Chemistry and Physics 212 (2018) 403–407

Contents lists available at ScienceDirect

Materials Chemistry and Physics

journal homepage: www.elsevier.com/locate/matchemphys

Materials science communication

TiO_2/Cu_2O coupled oxide films in Cl^- ion containing solution: Volta potential and electronic properties characterization by scanning probe microscopy

Ehsan Rahimi [a], Ali Rafsanjani-Abbasi [a], Amin Imani [b], Ali Davoodi [a, *]

[a] Materials and Metallurgical Engineering Department, Faculty of Engineering, Ferdowsi University of Mashhad, Azadi Square, Mashhad 91775-1111, Iran
[b] Materials and Polymers Engineering Department, Hakim Sabzevari University, Towhid-shahr, Sabzevar 9617976487, Iran

HIGHLIGHTS

- An accurate correlation between STS data and Volta potential of oxidized Ti/Cu couple was explained.
- TiO_2 matrix has higher Volta potential and energy band gap in comparison to Cu_2O.
- Formation of oxide compounds with new arrangement of energy levels detected after immersion test.
- TiO_2 becomes the nobler component of the galvanic couple over the time in 0.6 M NaCl electrolyte.

GRAPHICAL ABSTRACT

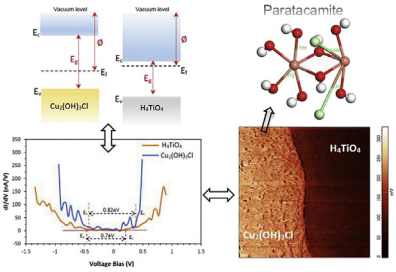

ARTICLE INFO

Article history:
Received 10 December 2017
Received in revised form
20 February 2018
Accepted 24 March 2018
Available online 26 March 2018

Keywords:
TiO_2/Cu_2O oxides
Volta potential
Density of states
Paratacamite
Scanning probe microscopy

ABSTRACT

In this study, a combination of scanning tunneling microscopy (STM), scanning tunneling spectroscopy (STS), atomic force microscopy (AFM), scanning Kelvin probe force microscopy (SKPFM), and density functional theory is applied to investigate the evolution of Volta potential and electronic properties of TiO_2/Cu_2O coupled oxides in presence of chloride-containing corrosive solution. Volta potential and the band gap of Cu_2O are increased in presence of chloride ion due to paratacamite ($Cu_2(OH)_3Cl$) formation whereas the opposite is seen for TiO_2 due to the formation of H_4TiO_4. The results shows a good correlation between the measured Volta potential difference and the observed corrosion behavior.

1. Introduction

Metal oxide surfaces are one of the most widely investigated topics in physics, chemistry, and materials science due to their fundamental importance in applications such as catalysis, microelectronics, magnetic storage media, and especially protective coatings against corrosion [1–3]. Meanwhile, many studies have focused intensively on the formation mechanisms, surface energies and electronic properties of oxide films on Ti and Cu pure metals in different media and conditions by transmission electron microscopy (TEM), atomic force microscopy (AFM), scanning tunneling microscopy (STM) and ultraviolet photoemission spectroscopy (UPS) [4–6].

TiO_2 is the most stable oxide of titanium and has an outstanding

* Corresponding author.
E-mail address: a.davodi@um.ac.ir (A. Davoodi).

https://doi.org/10.1016/j.matchemphys.2018.03.066
0254-0584/

resistance to corrosion and photocorrosion in atmospheric and aqueous environments in comparison with other semiconductor oxides [7]. Also, copper with high electrical and thermal conductivity slowly oxidizes in contact with an atmospheric ambient. Cuprous oxide (Cu_2O) is the most common initial corrosion product of the copper [8]. Thus, association of properties of both oxides can provide multiple necessities of good corrosion resistance and high thermal and electrical conductivity for specific applications such as aerospace, electronics, electrochemical and metallurgical equipment [9,10]. Despite numerous experimental and theoretical studies on titanium and copper oxides, there are limited data available evaluating the solid-liquid interface and electronic properties of these types of oxides as a function of time in the vicinity of each other [6]. In the case where a complete connection is available between oxides, many changes could be happened to the Volta potential, electronic property and galvanic interactivity between both oxides. Simultaneous responses of both oxides to gas or liquid media have severe effects on the adsorption mechanism and reactivity of the adsorbates on their surfaces [4,7,11–13].

In this study, multi-technical analysis including atomic force microscopy (AFM), scanning Kelvin probe force microscopy (SKPFM), scanning tunneling microscopy (STM) and scanning tunneling spectroscopy (STS) was performed in order to have a deeper understanding of electrochemical nobility and the density of states on TiO_2/Cu_2O surface. The distribution of the Volta potential along with the normalized differential conductance (dI/dV) extracted from the I-V curves of STS which are proportional to the surface density of electronic states [14–16].

2. Experimental

To produce a TiO_2/Cu_2O coupled sample, an industrial explosively welded pure Ti-Cu bimetal sheet was used. The flyer plate in the explosively joint sample is Ti sheet with a thickness of 3 mm and the base plate is a copper sheet with a thickness of 27 mm. The sample was received as a large plate with a size of $200 \times 200 \times 30$ mm. A massive specimen of Ti-Cu bimetal was cut into a cube for STM/STS and AFM/SKPFM analysis with a surface area of 1.25 cm^2. The specimen was ground with SiC paper up to 3000 grit, polished and ultrasonically cleaned in ethanol. Two automatically interchangeable measuring heads (SKPFM and STM), which are integrated into the Solver Next AFM instrument, were used. An n-doped silicon pyramidally-shaped tip was used for all SKPFM measurements. SKPFM measurements were performed in amplitude modulation (tapping mode) at ambient temperature with relative humidity of 25%, pixel resolution of 512×512 and scan frequency rate of 0.3 Hz. For STM/STS measurements, Pt–Ir tip was sharpened by cut-and-pull technique at about 60° angle with a special cutting scissor. The tip-sample distance was fixed by applying a constant bias voltage of 1 V and a set point current of 0.4 nA. In order to investigate the normalized differential conductance spectra, the tunneling currents were recorded in the scanning voltage range of −1.5 V to +1.5 V with a scanning rate of 400 mV/s. In order to perform the quantum chemical calculations of paratacamite, DMol3 modulus based on density function theory (DFT) in “Materials Studio 5.0” software was employed for investigation of Quantum chemical parameters such as the highest occupied molecular orbital (HOMO) and the lowest unoccupied molecular orbital (LUMO).

Galvanic measurement of TiO_2/Cu_2O couple was carried out in two separate electrodes with same area (1 cm^2) in 0.6M NaCl solution for investigation of the polarity reversal time. Galvanic experiments and potentiodynamic polarization measurement were performed with a Gill AC potentiostat (ACM) along with a saturated calomel electrode (SCE) and a platinum foil used as the reference and counter electrode, respectively.

3. Results and discussion

3.1. SKPFM and STS investigations

A schematically illustration for the energy-level diagram of TiO_2 and Cu_2O oxides is illustrated in Fig. 1a using analysis of SKPFM mapping (Fig. 1b) and STS data (Fig. 1f) of STM images (Fig. 1d and e). SKPFM image showed that the highest value of Volta potential is related to TiO_2 matrix with the mean value of 400 mV while the lowest value corresponds to Cu_2O matrix with the mean value of 52 mV. This large Volta potential value difference (Fig. 1c) or driving force ($\Delta V = 348$ mV) indicates the difference in work function values which is equivalent to their difference in Fermi level position in non-contact state [17,18]. In fact, Cu_2O has the Fermi level (E_f) close to the conduction band (E_c) while the Fermi level of TiO_2 is near to valence band (E_v), as shown in Fig. 1f which is similar to UPS band edges results of Greiner et al. [3].

The minimum density of states is assigned to the surface electronic gap (E_g) of the oxide films. TiO_2 and Cu_2O show band gap values of 2.1 eV and 0.5 eV along with steeply rising lines in Fig. 1f which are lower than expected values for the bulk oxide films (3.2 eV and 2.17eV, respectively) due to the presence of different surface states (or surface defects) [3,19,20]. Total tunneling current depends on the number of surface electronic states because the presence of numerous surface states (peaks) regarding surface defects and other adsorbates from the air (surface adsorbed OH^-) increases the specific surface area of the oxide films which leads to act as the new electronic states for electron tunneling [15,21].

Oxide films with more n-type conductivity exhibit larger tunneling current at negative sample bias voltages in I–V or dI/dV-V curves in comparison to positive sample bias voltages. The ratio between tunneling charge of occupied states and unoccupied states of the oxide surface can be used as n-type or p-type semiconductor character [22]. According to Fig. 1f, TiO_2 and Cu_2O show high charge ratio along with higher tunneling current at negative bias voltages which means that both oxides have more n-type semiconductor character. The work functions of most noble materials are usually higher than those with lower nobility [14,17]. As a result, TiO_2 behaves as the noble site during immersion in the electrolyte, while Cu_2O behaves like the active region which finally leads to the net flow of electrons from Cu_2O to TiO_2, as shown in Fig. 1c. In fact, the Volta potential distribution on metal oxide surface has usually been detected in air using SKPFM technique and its value depends on the work function of the metal oxide, surface condition and environmental conditions [21,23]. So, high value of work function and Volta potential indicate a high electrochemical nobility and it can be considered as a criterion for prediction of corrosion behavior [23].

The surface electronic properties of Cu_2O and TiO_2 are important because the surface conductivity is the important quantity for electrochemical activity. An increase in work function of TiO_2 reflects a higher stability of valence electrons leading enhanced resistance to corrosion attack in comparison with Cu_2O because a more stable electron state in TiO_2 limits valence electrons to participate in electrochemical reactions [24]. Also, the low value of Volta potential or work function on Cu_2O in comparison with TiO_2 can be explained as an increasing tendency for electron transfer. Therefore, Cu_2O in the electrolyte media could be susceptible for more corrosion attacks and anodic electrochemical reactions.

During immersion of the TiO_2/Cu_2O coupled sample in 0.6 M NaCl solution for 3600 s, a noticeable evolution observed in the microstructure, Volta potential and electronic properties of both. SKPFM analysis showed that the Volta potential distribution on TiO_2/Cu_2O changed along with the formation of new oxide films.

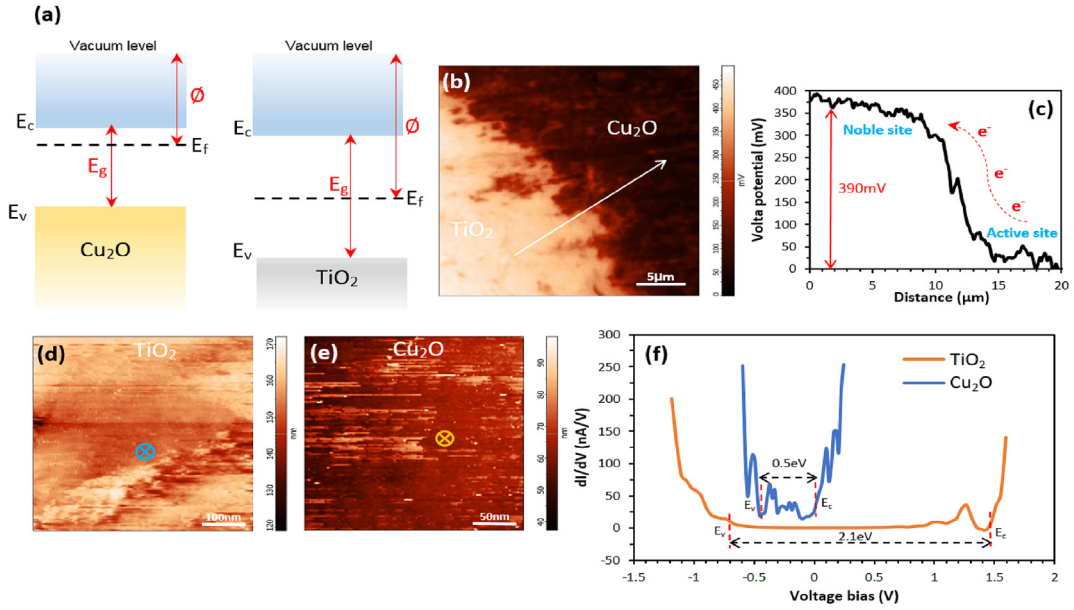

Fig. 1. (a) Schematic illustration of the energy levels for Cu_2O and TiO_2 oxides, (b) Volta potential map and (c) Volta potential line profile of TiO_2/Cu_2O oxides of the line shown in (b), (d,e) STM images of TiO_2 and Cu_2O (1 V voltage bias, 0.4 nA current tunneling), (f) differential conductance spectra numerically obtained from the STS curve (I-V) for TiO_2 and Cu_2O. All experiments were performed in 27°C and relative humidity of 27%±1.

Cu_2O during interaction with chloride ion results in the formation of nantokite (CuCl) which commonly transforms to atacamite or the isomorphous phase paratacamite ($Cu_2(OH)_3Cl$) [8,25]. The reactivity of n-type TiO_2 and water along with dissolved oxygen and chloride ions involves various processes at TiO_2/H_2O interface which leads to the formation of chemisorbed species in the adsorbed layer and changes in the lattice defect disorder [7]. The interaction of TiO_2 with H^+ (due to decomposition of H_2O in an adsorbed layer on TiO_2 surface) may lead to the removal of oxygen vacancies in TiO_2 lattice and finally leads to the formation of a low dimensional H_4TiO_4 surface structure [7]. Therefore, the lowest Volta potential is related to H_4TiO_4 and the highest value of it correspond to $Cu_2(OH)_3Cl$ (Fig. 2b and c).

Scanning tunneling spectroscopy on TiO_2 surface immersed in 0.6 M NaCl solution depicts a decreased surface electronic gap while this was the reverse for Cu_2O. The occupied and unoccupied states have significantly increased for H_4TiO_4 which indicates that TiO_2 vacancies are frequently considered as an acceptor-type of

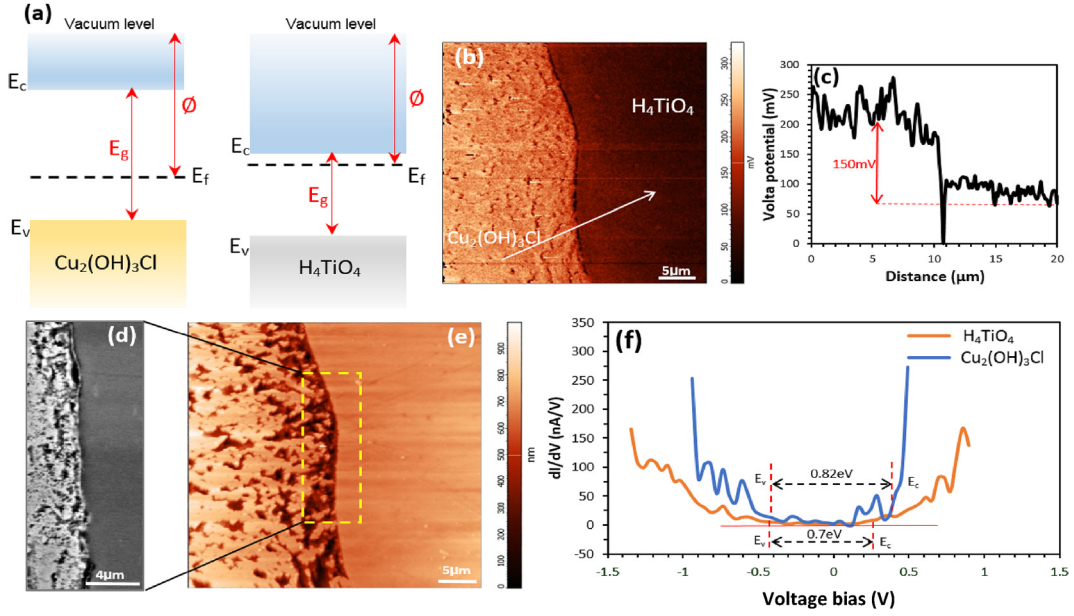

Fig. 2. (a) Schematic energy levels of $Cu_2(OH)_3Cl$ and H_4TiO_4 oxides extracted by SKPFM and STS after interaction with 0.6 M NaCl solution for 3600 s, (b) Volta potential maps and (c) line profile of $Cu_2(OH)_3Cl/H_4TiO_4$, (d,e) SEM and AFM images of TiO_2/Cu_2O coupled oxide after immersion in 0.6 M NaCl solution for 3600 s, and (f) differential conductance spectra numerically obtained from the STS curve (I-V) for $Cu_2(OH)_3Cl$ and H_4TiO_2. All experiments were performed at ambient temperature and relative humidity of 27%±1.

foreign defects such as H^+ [7]. Also, it can be observed that the value of conduction band energy for H_4TiO_4 ($E_c = 0.2eV$) is lower than TiO_2 ($E_c = 1.2eV$) due to a significant increase of unoccupied surface states. Subsequently, the density of surface states on $Cu_2(OH)_3Cl$ matrix is decreased in the occupied and unoccupied states in comparison with Cu_2O due to the formation of oxide compounds with new energy level arrangement.

3.2. DFT calculation

Paratacamite and atacamite have the same chemical composition but paratacamite with trigonal crystal system is the most probable corrosion product of Cu_2O in comparison to atacamite with orthorhombic crystal system during interaction with NaCl solution [26]. Fig. 3 shows the molecular structure of paratacamite which was calculated using DFT. According to DFT calculation and frontier molecular orbital theory, three quantum chemical parameters of paratacamite can be defined including the energy of the highest occupied molecular orbital ($E_{HOMO} = -8.748eV$), energy of the lowest unoccupied molecular orbital ($E_{LUMO} = -5.571eV$) and band gap energy ($\Delta E = E_{LUMO} - E_{HOMO} = 3.177eV$) [27]. The surface electronic gap value of $Cu_2(OH)_3Cl$ from STS data is lower than the DFT calculation because in STS the density of occupied and unoccupied states of $Cu_2(OH)_3Cl$ surface will be considered as a real condition.

3.3. Electrochemical measurements

Fig. 2d and e shows SEM and topography images as direct evidences for Volta potential mapping predictions. Post-exposure examinations of the surface in an SEM image confirmed that less noble sites which have been previously indicated by SKPFM Volta potential assessment, are electrochemically anodic. Therefore, in a galvanic corrosion, TiO_2 will be a site with higher Volta potential in comparison to Cu_2O.

In order to investigate the galvanic corrosion between TiO_2 and Cu_2O oxide films after immersion in the Cl^- containing electrolyte, galvanic measurements were performed (Fig. 4). A dramatic increase in current and potential in the beginning of the measurements was observed which indicates the formation of an oxide film on Ti side. The noble behavior of TiO_2 in electrochemical measurements is incomparable with SKPFM mapping results because in the electrochemical measurements the metal/oxide/electrolyte interfaces are considered while the focus of SKPFM is on oxide/air interface [1,14]. In addition, a space charge similar to a Gouy-Chapman diffuse region forms by a rearrangement of the charge carriers brought about by the intense field caused by the interaction of the ionic conductors [28]. Therefore, a special difference exists in the oxide/air interface in SKPFM technique and oxide/electrolyte interface in electrochemical measurement. According to the galvanic current curves in Fig. 4, negative galvanic current values

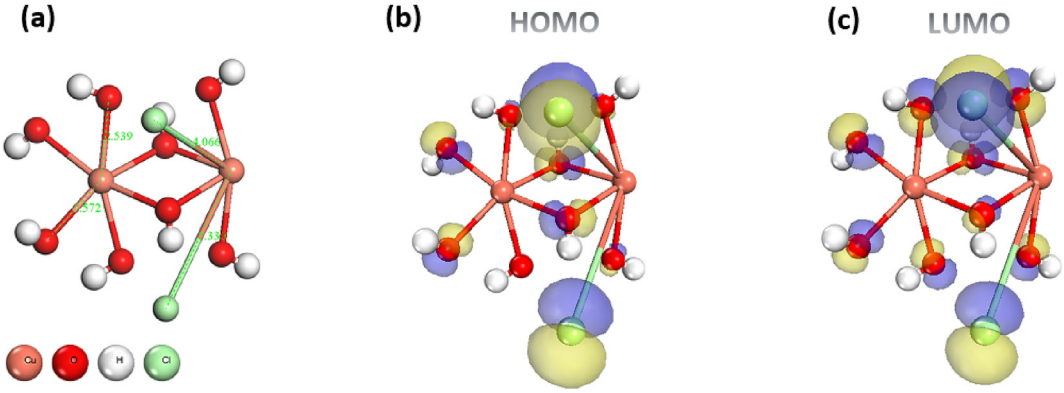

Fig. 3. (a) Optimized geometry of paratacamite ($Cu_2(OH)_3Cl$), (b) HOMO orbitals, (c) LUMO orbitals.

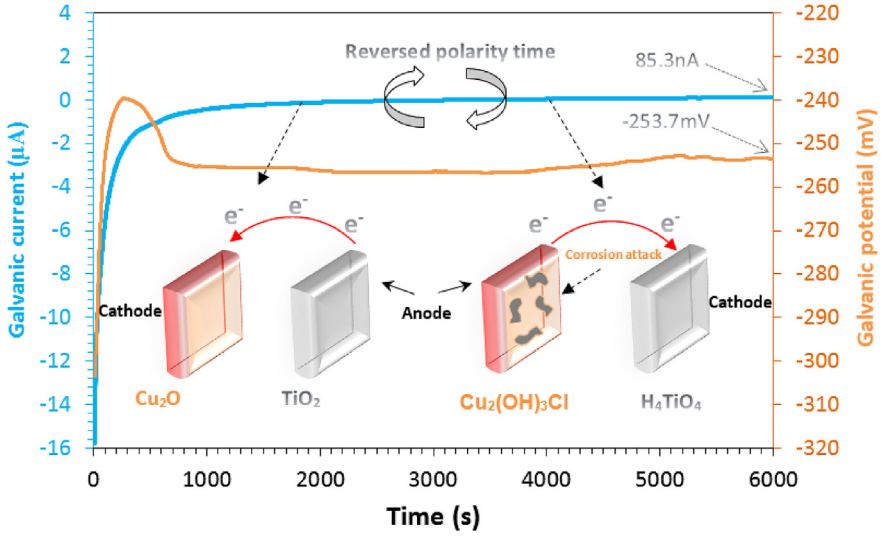

Fig. 4. Galvanically polarized current and potential measurements of Ti/Cu couple obtained after interaction with 0.6 M NaCl solution in ambient temperature for 6000 s.

below the zero galvanic current indicate the net flow of electrons from TiO_2 with anodic behavior to Cu_2O with cathodic behavior [29]. In addition, a gradual increasing can be observed at first moments of immersion of TiO_2/Cu_2O coupled oxides in the galvanic potential curve. In fact, the rapid and more growth of TiO_2 film leads to higher corrosion resistance and the tendency for cathodic behavior.

Polarity reversal will happen after approximately 3000 s and the net flow of electrons invert from Cu_2O to TiO_2 because a new dense oxide film presents on the surface with different properties. A video of this process (5x times speeded down) is provided by potentiodynamic polarization test which is available in the online version of this article (Video 1).

Supplementary video related to this article can be found at https://doi.org/10.1016/j.matchemphys.2018.03.066.

4. Conclusions

In summary, Volta potential and electronic properties of TiO_2/Cu_2O coupled oxides in presence of chloride-containing corrosive solution investigated by STM/STS and AFM/SKPFM multi-technical analysis. SKPFM and STS investigations well demonstrated the Volta potential and band edges during interactions on TiO_2/Cu_2O surface in presence of the chloride-containing corrosive solution. Volta potential and the band gap of Cu_2O increased in presence of chloride ion regarding paratacamite ($Cu_2(OH)_3Cl$) formation while this was the reverse for TiO_2 due to the formation of H_4TiO_4. AFM and SEM images clearly demonstrated that the severe corrosion attack in Cu_2O side which agrees with Volta potential maps. Results showed an accurate correlation between STS data and Volta potential which in turn provide a new viewpoint for TiO_2/Cu_2O coupled oxides to be used simultaneously in multifunctional applications such as providing good corrosion resistance and high thermal and electrical conductivity.

Acknowledgment

Hakim Sabzevari University and Ferdowsi University of Mashhad are appreciated for providing AFM/SKPFM, STM/STS, and SEM characterization.

References

[1] A. Picone, M. Riva, A. Brambilla, A. Calloni, G. Bussetti, M. Finazzi, F. Ciccacci, L. Duò, Reactive metal–oxide interfaces: a microscopic view, Surf. Sci. Rep. 71 (2016) 32–76.
[2] G. Lu, S.L. Bernasek, J. Schwartz, Oxidation of a polycrystalline titanium surface by oxygen and water, Surf. Sci. 458 (2000) 80–90.
[3] M.T. Greiner, M.G. Helander, W.-M. Tang, Z.-B. Wang, J. Qiu, Z.-H. Lu, Universal energy-level alignment of molecules on metal oxides, Nat. Mater. 11 (2012) 76–81.
[4] J. Lee, D.C. Sorescu, X. Deng, K.D. Jordan, Water chain formation on TiO_2 (110), J. Phys. Chem. Lett. 4 (2012) 53–57.
[5] S. Tan, Y. Ji, Y. Zhao, A. Zhao, B. Wang, J. Yang, J. Hou, Molecular oxygen adsorption behaviors on the rutile TiO_2 (110)-1× 1 surface: an in situ study with low-temperature scanning tunneling microscopy, J. Am. Chem. Soc. 133 (2011) 2002–2009.
[6] J. Kunze, V. Maurice, L.H. Klein, H.-H. Strehblow, P. Marcus, In situ scanning tunneling microscopy study of the anodic oxidation of Cu (111) in 0.1 M NaOH, J. Phys. Chem. B 105 (2001) 4263–4269.
[7] J. Nowotny, T. Norby, T. Bak, Reactivity between titanium dioxide and water at elevated temperatures, J. Phys. Chem. C 114 (2010) 18215–18221.
[8] X. Zhang, I. Odnevall Wallinder, C. Leygraf, Mechanistic studies of corrosion product flaking on copper and copper-based alloys in marine environments, Corrosion Sci. 85 (2014) 15–25.
[9] F. Findik, Recent developments in explosive welding, Mater. Des. 32 (2011) 1081–1093.
[10] I. Bataev, D. Lazurenko, S. Tanaka, K. Hokamoto, A. Bataev, Y. Guo, A. Jorge Jr., High cooling rates and metastable phases at the interfaces of explosively welded materials, Acta Mater. 135 (2017) 277–289.
[11] A. Soon, M. Todorova, B. Delley, C. Stampfl, Thermodynamic stability and structure of copper oxide surfaces: a first-principles investigation, Phys. Rev. B 75 (2007), 125420.
[12] J.W. Schultze, M. Lohrengel, Stability, reactivity and breakdown of passive films. Problems of recent and future research, Electrochim. Acta 45 (2000) 2499–2513.
[13] Z. Hua, B. An, T. Iijima, C. Gu, J. Zheng, The finding of crystallographic orientation dependence of hydrogen diffusion in austenitic stainless steel by scanning Kelvin probe force microscopy, Scripta Mater. 131 (2017) 47–50.
[14] C. Barth, A.S. Foster, C.R. Henry, A.L. Shluger, Recent trends in surface characterization and chemistry with high-resolution scanning force methods, Adv. Mater. 23 (2011) 477–501.
[15] Y. Lin, R. Lin, W. Wang, X. Xiao, Characterization of TiO_2 nanocrystalline thin film by scanning tunneling microscopy and scanning tunneling spectroscopy, Appl. Surf. Sci. 143 (1999) 169–173.
[16] O. Wolf, M. Dasog, Z. Yang, I. Balberg, J. Veinot, O. Millo, Doping and quantum confinement effects in single si nanocrystals observed by scanning tunneling spectroscopy, Nano Lett. 13 (2013) 2516–2521.
[17] M. Rohwerder, F. Turcu, High-resolution Kelvin probe microscopy in corrosion science: scanning Kelvin probe force microscopy (SKPFM) versus classical scanning Kelvin probe (SKP), Electrochim. Acta 53 (2007) 290–299.
[18] J. Umeda, N. Nakanishi, K. Kondoh, H. Imai, Surface potential analysis on initial galvanic corrosion of Ti/Mg-Al dissimilar material, Mater. Chem. Phys. 179 (2016) 5–9.
[19] A. Borodin, M. Reichling, Characterizing TiO_2 (110) surface states by their work function, Phys. Chem. Chem. Phys. 13 (2011) 15442–15447.
[20] M. Okada, L. Vattuone, K. Moritani, L. Savio, Y. Teraoka, T. Kasai, M. Rocca, X-ray photoemission study of the temperature-dependent CuO formation on Cu (410) using an energetic O_2 molecular beam, Phys. Rev. B 75 (2007), 233413.
[21] T. Massoud, V. Maurice, F. Wiame, L.H. Klein, A. Seyeux, P. Marcus, Local electronic properties of the passive film on nickel studied by scanning tunneling spectroscopy, J. Electrochem. Soc. 159 (2012) C351–C356.
[22] T. Knutsen, S. Diplas, T. Våland, S. Jørgensen, T. Norby, A study of anodically grown hydroxide films on an amorphous Ni78Si8B14 alloy, J. Electrochem. Soc. 154 (2007) F111–F121.
[23] C. Örnek, D. Engelberg, SKPFM measured Volta potential correlated with strain localisation in microstructure to understand corrosion susceptibility of cold-rolled grade 2205 duplex stainless steel, Corrosion Sci. 99 (2015) 164–171.
[24] L. Guo, G. Hua, B. Yang, H. Lu, L. Qiao, X. Yan, D. Li, Electron work functions of ferrite and austenite phases in a duplex stainless steel and their adhesive forces with AFM silicon probe, Sci. Rep. 6 (2016) 20660.
[25] H. Lin, G. Frankel, Atmospheric corrosion of cu during constant deposition of NaCl, J. Electrochem. Soc. 160 (2013) C336–C344.
[26] J. Boita, M. do Carmo Martins Alves, J. Morais, A reaction cell for time-resolved in situ XAS studies during wet chemical synthesis: the $Cu_2(OH)_3Cl$ case, J. Synchrotron Radiat. 21 (2014) 254–258.
[27] Y. Zhu, M.L. Free, G. Yi, The effects of surfactant concentration, adsorption, aggregation, and solution conditions on steel corrosion inhibition and associated modeling in aqueous media, Corrosion Sci. 102 (2016) 233–250.
[28] K. Oldham, J. Myland, A. Bond, Electrochemical Science and Technology: Fundamentals and Applications, John Wiley & Sons, 2011.
[29] U. Donatus, G.E. Thompson, X. Zhou, Effect of near-ambient temperature changes on the galvanic corrosion of an AA2024-T3 and mild steel couple, J. Electrochem. Soc. 162 (2015) C42–C46.